Photocarrier Escape Time in Quantum-Well Light-Absorbing Devices: Effects of Electric Field and Well Parameters

Valentin V. Nikolaev and Eugene A. Avrutin, *Member, IEEE*

***Abstract*—We analyze the dependence of the carrier escape time from a single-quantum-well optoelectronic device on the aplied electric field and well width and depth. For this purpose, a new simple and computationally efficient theory is developed. This theory is accurate in the case of electrons, and the assessment of the applicability for holes is given. Semi-analytical expressions for the escape times are derived. Calculations are compared to experimental results and previous numerical simulations. Significant correlations between the position of quantum-well energy levels and the value of the escape time are found. The main escape mechanism at room temperature is established to be thermally assisted tunneling/emission through near-barrier-edge states. The formation of a new eigenstate in the near-barrier-edge energy region is found to reduce the electron escape time significantly, which can be used for practical device optimization.**

***Index Terms*—Optoelectronic devices, quantum wells (QWs), saturable absorbers.**

I. Introduction

THERE is a significant number of semiconductor devices which contain reverse-biased quantum wells (QWs), such as optical modulators [1], photodetectors [2], photovoltaic devices. Saturable absorbers (SAs), usually also based on reverse-biased QWs, are used in such devices as mode-locked lasers [3] and all-optical signal-processing devices [4]–[6].

One of the most important characteristics of such devices is the time in which the reverse-biased section recovers from the saturated state back into the absorbing state. In some cases, this characteristic time constant determines the limiting operational frequency of the device. It is desirable to lower the recovery time down to single picoseconds while retaining other important device characteristics. Therefore, a thorough understanding of the carrier escape processes is crucial for a proper optimization of device parameters.

Two processes contribute to carrier escape from a semiconductor QW in an electric field: the tunneling of the carriers through the barrier and the thermionic emission above the barrier. A simple model of thermionic emission was developed by Schneider and von Klitzing [7]. This model uses three-dimensional (3-D) density of states to describe above-barrier states; no above-barrier reflection is taken into account and the barrier height is a fitting parameter which is not fixed to the positions of the size-quantized levels. Consequently, the model is essentially three-dimensional, which limits its application for quantitative analysis of real quasi-two-dimensional structures. Despite this, the simplicity of this approach led to its being widely used for evaluation of the thermionic escape time.

Several methods of calculation of the carrier tunneling time from QWs has been developed using various degrees of approximation [2], [8]–[10]. In all of these papers, tunneling is considered as taking place solely from quasi-bound states of the QW, which are essentially two-dimensional (2-D) states with a finite but extremely narrow broadening caused by barrier penetration (tunneling escape). Such an approach is justifiable only for well-bound states with long tunneling times; it cannot describe the escape from weakly bound states, which occurs in QWs in a sufficiently strong electric field.

There were attempts to apply the combination of quasi-2-D tunneling and 3-D thermionic emission approaches to describe the total escape time from QW structures [11], [12]. However, it is clear that a QW in an electric field is, strictly speaking, neither a quasi-2-D nor a fully 3-D system. Variation of the electric field and the parameters of the QW can cause transformations of QW states from quasi-2-D to 3-D, which remained unaccounted for by the simple 2-D/3-D-combination approach.

The most recent theoretical development in the field, presented by Anwar and Lefebvre [13], [14], is an advance compared to the previous theories in that it treats thermionic emission and tunneling on the same footing. This theoretical approach stems from quantum kinetic theory [15], which uses Green's function technique to calculate the local density of states $\rho_{Ez}(z)$ and the local group velocity $v_{Ez}(z)$, where E_z is the energy parameter [16]. However, finding the value of electron escape time by the method of [13] and [14] constitutes a formidable numerical task. Namely, to find $\rho_{Ez}(z)$ and $v_{Ez}(z)$, one has to integrate a first-order differential equation, where E_z varies in the appropriate energy interval. Then, one should perform averaging over the QW width and integrate the averaged quantities over energy E_z. This precludes obtaining analytical expressions even for a single-QW system. The purely numerical nature of this approach and its computational complexity hinder its use for analysis of different structures. In addition, approximating the carrier probability flux inside the QW using *the effective carrier velocity*—a local carrier group velocity averaged over the QW width, although pretty accurate in some cases [13]—may run into trouble for shallow QWs, large applied fields, or in the case of more complex structures

Manuscript received February 20, 2003; revised May 22, 2003. This work was supported by U.K. Engineering and Physical Sciences Research Council (EPSRC) under Grant GR/R84238/01.

The authors are with the Department of Electronics, University of York, Heslington, York YO10 5DD, U.K.

Digital Object Identifier 10.1109/JQE.2003.819527

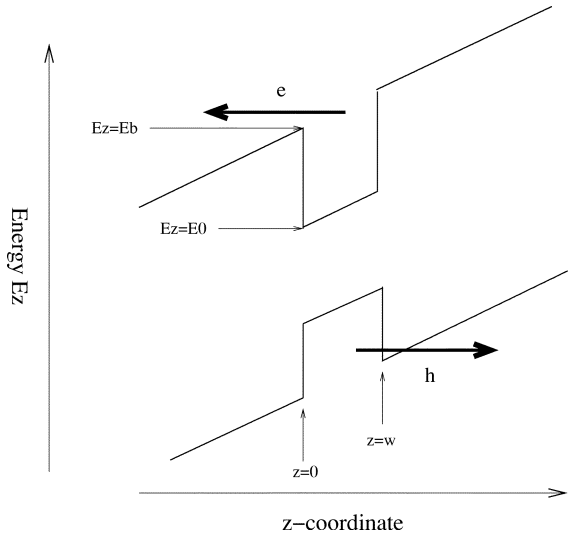

Fig. 1. Schematic conduction and valence band structure.

comprising multiple QWs or gradient layers, where the concept of the QW width is not well established.

To the best of our knowledge, no thorough study of the dependence of the carrier escape on the QW parameters and the analysis of the escape mechanisms has yet been performed. In this paper, we aim to do this using a new, computationally efficient way of evaluating carrier escape time from a single QW under an arbitrarily strong reverse bias. The current density of carriers escaping from the QW is expressed analytically and the thermionic and tunneling components as well as the total value of the current are found by integration over appropriate energy intervals. The use of quantum mechanical reflection/transmission coefficients allows us to treat all the quasi-bound (below-barrier) and unbound (above-barrier) states on the same footing. Quasi-equilibrium between carrier states is assumed and the simple effective-mass approximation is used. The latter approximation is justified for electrons and so the theory is expected to be accurate in their case; its applicability in the case of holes is discussed in Section III-B. No additional approximations were involved, which makes for a more accurate theory compared to all the previous models.

II. Theory

We study carrier escape from a single QW (here, we consider GaAs) embedded in a large slab of bulk material—here, $Al_xGa_{1-x}As$. The electric field is applied along the structure growth axis z. As the thick arrows schematically depict in Fig. 1, photogenerated electrons and holes leave the QW by escaping in opposite directions. Each layer is assigned its in-plane and transverse effective masses. The in-plane carrier motion is described by a 2-D wavevector, and the envelope-wavefunction approximation can be used. For definiteness, let us assign the coordinate $z = 0$ to the left boundary of the QW and the coordinate $z = w$ to the right boundary. Below, we first consider a purely one-dimensional (1-D) situation describing electrons moving along the z-axis in a 1-D potential. Later, we will return to the 3-D system by evoking the in-plain degrees of freedom.

A. Escape Current

Let us analyze the set of wave functions that characterize the electronic system. In any homogeneous semiconductor layer in an electric field F, the electronic wave function ψ can be represented as a linear combination of two counterpropagating electronic waves $a(z)$ and $a^*(z)$ as

$$\psi = c_1 a(z) + c_2 a^*(z), \tag{1}$$

$$a(z) = \mathrm{Ai}(x) + j\mathrm{Bi}(x)$$

$$x = \left(\left[\frac{2m_e}{(e\hbar F)^2} \right]^{1/3} (eFz - E_z + V) \right) \tag{2}$$

where $\mathrm{Ai(x)}$ and $\mathrm{Bi(x)}$ are the Airy functions, m_e is the transverse effective mass of electrons in the layer, $\hbar$ is the Dirac constant, e is the modulus of the electronic charge, V is the layer's conduction band offset, and E_z is the electron energy.

By evaluating the probability flux i^a associated with $a(z)$ and using the Wronskian of the Airy differential equation [17], one can find

$$i^a = \frac{j\hbar}{2m_e} \left(a(z) \frac{d}{dz} a^*(z) - a^*(z) \frac{d}{dz} a(z) \right)$$

$$= \frac{1}{\pi} \left(\frac{2e\hbar F}{m_e^2} \right)^{1/3}. \tag{3}$$

This shows that the wavefunction $a(z)$ [see (2)] carries a constant probability flux along the z axis. Similarly, the probability current of the complex conjugate $a^*(z)$ flows in the opposite direction.

Now we introduce the (energy) density of the probability flux $i_E(E_z) = di/dE_z$, di being the probability flux of electron states with energies in an infinitesimal interval dE_z. Spin degeneracy is ignored for the time being. Generally, $i_E(E_z)$ will depend on the direction along the z axis and on the properties of a particular semiconductor layer. In a bulk semiconductor slab of width L (where L is large), the energy density of the probability flux is

$$i_{E0} = \frac{di_0}{dE_z} = v_0 \frac{1}{L} \frac{dN^+}{dE_z} = \frac{\hbar k_z}{m} \frac{1}{L} \frac{L}{2\pi} \frac{dk_z}{dE_z} = \frac{1}{2\hbar\pi} \tag{4}$$

where v_0 is the electron velocity and dN^+ is the number of states within the energy interval dE_z propagating in a given (here, positive) direction. As can be expected, i_{E0} does not depend on the layer width L nor on the energy $E_z = \hbar^2 k_z^2/2m$.

In order to get a set of electronic wavefunctions describing the system under consideration, we should use appropriate boundary conditions. It is clear that, in the case of an infinite structure, all the states can be considered as originating from electronic waves which propagate toward the structure from infinity (from the left in case of electrons) and experience reflection from the structure. This has no relation to the fact that in a real physical situation there is no electrons incident on the structure. As a boundary condition we chose the value of the density of the probability flux incident on the structure to be equal to $i_{E0} = (2\pi\hbar)^{-1}$ [see (4)]. The reasons for choosing this boundary condition can be seen from the following consideration. Since our single-QW structure has (infinitely) wide barrier layers, one can find a position far enough from the QW where the electronic states are undisturbed by the presence

of QW and have the same density and probability flux as in a homogeneous bulk material. By choosing such a boundary condition, we can construct a set of continuous wavefunctions.

To find the density of the probability flux inside the structure, we employ the formalism of propagating waves [see (1)] and reflection/transmission coefficients. The latter are determined as the ratios of the reflected/transmitted component of the wavefunction to the incident component; for example, the reflection for a left-propagating incident wave is characterized by $r^- = c_{10}a(z_0)/(c_{20}a^*(z_0))$ and the transmission from a point z_0 to $z_f > z_0$, by $t_{0f} = c_{1f}a(z_f)/(c_{10}a(z_0)) \times (|a(z_0)|m_0^{1/3})/(|a(z_f)|m_f^{1/3})$. Here, 0 ($f$) stands for the initial (final) point of propagation, and the additional factor in the expression for the transmission coefficient is in order to ensure that the squared modulus of the coefficient gives the ratio of the transmitted and incident probability fluxes. When calculating the value of the reflection coefficient r^+ of the right-propagating wave from an infinite impenetrable structure on the right-hand side of Fig. 1, the condition of vanishing of the wavefunction at infinity is used: $c_1 = c_2 = c$ in (1), i.e., $\psi(z) = c(a(z) + a^*(z)) = 2c\mathrm{Ai}(x)$ when $z \longrightarrow +\infty$

In this approach, the density of the probability flux inside the QW is the result of interference of all different processes which account for penetration of external probability current into the QW:

$$\begin{aligned} i_E^{\mathrm{QW}}(E_z) &= i_{E0}\left\|t + tr^+r^- + t(r^+r^-)^2 + \ldots\right\|^2 \\ &= \frac{|t|^2 i_{E0}}{|1 - r^+r^-|^2} \end{aligned} \tag{5}$$

where t is the transmission coefficient that describes the penetration of an electron from infinity to a point Z inside the QW, and r^+ and r^- are the reflection coefficients for an electron propagating from Z to the right (in the positive direction) and to the left (in the negative direction), respectively.

The procedure of finding the density of the probability flux inside the QW described above is rigorous and is equivalent to solving the Schrödinger equation with the appropriate boundary conditions.

The quantity $|t|^2$ gives the tunneling coefficient trough the potential barrier

$$|t|^2 = \frac{4}{\pi^2}\left(\frac{2\gamma eF}{(\hbar m_{\mathrm{QW}})^2}\right)^{2/3} \frac{[X^*(0-) - X(0+)]^{-2}}{|a(0+)a(0-)|^2} \tag{6}$$

where $X(z) = m^{-1}a'(z)/a(z)$; γ is the ratio of the QW transverse effective mass to the barrier effective mass $\gamma = m_{\mathrm{QW}}/m_B$, and $a(z)$ is given by (2).

For a wide and high enough barrier, one can use the asymptotic behavior of the Airy functions to obtain an approximate expression for the transmission coefficient

$$\begin{aligned} |t|^2 = &\frac{\sqrt{\gamma(E_z - E_0)(E_b - E_z)}}{\gamma(E_b - E_z) + (E_z - E_0)} \\ &\times \exp\left(-\frac{4}{3}\frac{\sqrt{2m}}{e\hbar F}(E_b - E_z)\right) \end{aligned} \tag{7}$$

where E_0 and E_b are, respectively, the minimum and maximum underbarrier tunneling energies, as shown in Fig. 1. The exponential function from (7) alone gives the quasi-classical (WKB) result. One can see that, even for a wide potential barrier, the actual tunneling coefficient differs from the WKB result by a pre-exponential factor that is, in general, not unity. The same relation between quasi-classical and exact results is found for tunneling through a rectangular potential barrier (see [18]).

For any point Z, $0 < Z < w$, inside the QW, the product of the reflection coefficients for waves incident from both sides can be decomposed into the following form:

$$r^+r^- = r_0 r_w \frac{a(w-)a^*(0+)}{a^*(w-)a(0+)} \tag{8}$$

where r_0 (r_w) is the reflection coefficient from the left (right) QW interface. Here $w-$ (0+) means taking in (2) $z = w$ ($z = 0$) and the band offset V and the effective mass m equal to that in the layer on the left (right) of the interface $z = w$ ($z = 0$), that is, of the QW. Note that the value given by (8) does not depend on the choice of the point Z inside the well.

The complex reflection coefficients from both QW boundaries are found in the following form:

$$r_0 = \frac{X^*(0+) - X^*(0-)}{X^*(0-) - X(0+)} \tag{9}$$

$$r_w = \frac{\mathrm{Re}[X(w+)a(w+)] - X(w-)\mathrm{Re}[a^*(w+)]}{X^*(w-)\mathrm{Re}[a^*(w+)] - \mathrm{Re}[X(w+)a(w+)]}. \tag{10}$$

As can be expected, $|r_w|^2 = 1$, that is, the electron escape along the positive z direction is prohibited.

Having established the density of the probability flux due to electron wavefunctions, we can now find the value of the energy density of the particle flux along the z axis, provided that the carrier distribution over different states inside the QW is known. The density of the particle flux inside the QW is

$$j_E^{\mathrm{QW}}(E_z) = i_E^{\mathrm{QW}}(E_z) \times \frac{2}{S}\sum_{k_{||}} f_{Ez,k_{||}} = i_E^{\mathrm{QW}}(E_z)P(E_z) \tag{11}$$

where S is the device area, $k_{||}$ is the in-plane wavevector, and f is the distribution function. The physical meaning of the factor $P(E)$ introduced in (11) is such that, for any quasi-bound level E^{QB}, $P(E^{\mathrm{QB}})$ is the density of electrons on this level.

In this paper, we assume that electrons inside the QW are in the state of quasi-equilibrium described by the quasi-Fermi level μ_e. In this case, we have

$$\begin{aligned} P(E) &= 2\int \frac{dk^2}{(2\pi)^2} f_e\left(\frac{\hbar^2k^2}{2m_{||}} + E\right) \\ &= \frac{m_{||}}{\beta\hbar^2\pi}\ln\left(1 + \exp(\beta(\mu_e - E))\right) \end{aligned} \tag{12}$$

where $m_{||}$ is the electron in-plane effective mass and $f_e(E) = [\exp(\beta(E - \mu_e)) + 1]$ is the Fermi distribution function, β is the inverse temperature measured in energy units, and the spin degeneracy is taken into account by the factor of two.

The energy density of the flux of particles escaping out of the structure is given by multiplying the internal current [(11)] by the transmission coefficient $|t|^2$. Finally, the total

escape current density is given by the integral over energy $J = e\int_{E_0}^{\infty} j_E(E_z)\,dE_z$, where

$$j_E(E_z) = \frac{1}{2\hbar\pi}\frac{|t(E_z)|^4 P(E_z)}{|1 - r_+ r_-(E_z)|^2}. \tag{13}$$

Thus, we have obtained an analytical expression for the escape current density from a single-QW structure, with no additional approximations. To calculate the rigorously determined escape current density [(13)], one has to combine (1), (6), and (8)–(10). From the computational point of view, this involves nothing more complicated than evaluating Airy functions of purely real arguments.

B. Quasi-Bound States

If the electric field F is not too large, the tunneling coefficient, (6) or (7), is very small in a certain energy region, and, since the transmission and reflection coefficients are related by the probability flux conservation law $|t|^2 + |r_-|^2 = 1$, the modulus of the reflection coefficient product $r_+ r_-$ is close to unity. It is clear from (13) that in this situation sharp peaks in the current density will occur at energies where the product $r_+ r_-$ becomes real and positive. These sharp current density peaks correspond to quasi-bound states of electrons in the QW. From (8), the eigenvalue equation for the energies of these size-quantized states is

$$\begin{aligned}\arg(r_+ r_-(E_s^{\mathrm{QB}})) =& \arg(r_0) + \arg(r_w) + 2\arg\left(\frac{a(w-)}{a(0+)}\right)\\ =& 2\pi s\end{aligned} \tag{14}$$

where $s = 0, 1, 2\ldots$

By linearizing the dependences of phases of the coefficients in (13) in the vicinity of a quasi-bound level E_s^{QB} and using the probability conservation law, one can obtain an approximate expression for the current density in the vicinity of the quasi-bound state

$$\begin{aligned} j_E(E_z) &= \frac{|r_0|^{-1}\Delta^{-1}|t|^4}{2\hbar(1-|r_0|)}\lambda\left(\frac{1-|r_0|}{|r_0|\Delta}; E - E_s^{\mathrm{QB}}\right) P(E_s^{\mathrm{QB}})\\ &\approx \frac{|t|^2}{\hbar\Delta}\lambda\left(\frac{|t|^2}{2\Delta}; E - E_s^{\mathrm{QB}}\right) P(E_s^{\mathrm{QB}}),\end{aligned} \tag{15}$$

where $\lambda(\sigma; x) = \pi^{-1}\sigma/(x^2 + \sigma^2)$ is the Lorentz function and $\Delta = |d(\arg(r^+ r^-))/dE_z|$ is the modulus of the energy derivative of the sum of phases in the left-hand side of (14). The derivative and the values $|t|^2$ and $|r_0|$ are taken at $E_z = E_s^{\mathrm{QB}}$. This expression is valid if $|t|^2$ is small, i.e., the flux peak is narrow.

Under this condition of the tunneling coefficient being small, the quasi-bound states are well described by a step-like 2-D density of states, and the density of the carriers residing on the quasi-bound level is simply $n_s^{\mathrm{QB}} = P(E_s^{\mathrm{QB}})$, where P is given by (12). By definition, the time of tunneling from a quasi-bound level is given by

$$\frac{1}{\tau_s^{\mathrm{QB}}} = \frac{\int j_E(E_z)\,dE_z}{n_s^{\mathrm{QB}}} = \frac{|t|^2}{\hbar|\Delta|}. \tag{16}$$

Here, integration over energy E_z is performed in the vicinity of the quasi-bound level. It is evident that evaluating Δ and $|t|^2$ at the quasi-bound level provides an efficient method for calculation of the tunneling time.

By analogy with the previously used approaches for evaluation of the time of tunneling escape from a quasi-bound level [2], [10], we can introduce the frequency of carrier collisions with the barrier $\omega = 2\pi/T$, where T is "the period of oscillation"

$$\begin{aligned} T =& \hbar|\Delta|\\ =& -\hbar\frac{d}{dE_z}\left(\arg(r_0) + \arg(r_w) + 2\arg\left(\frac{a(w-)}{a(0+)}\right)\right).\end{aligned} \tag{17}$$

Those parts of T which are due to the reflection coefficients r_0 and r_w can be interpreted as the times spent by a carrier under the corresponding barrier, and the third term in (17) is due to carrier travel from one interface to the other and back. Using the asymptotics of the Airy functions, one can show that, in the case of a low electric field and a high enough barrier, the reflection coefficients are approximately $r_0 \approx -1$, $r_w \approx -1$, and so the simple expression for the oscillation period of the electron on the sth level in infinitely-deep QWs [2], [10], $T = 2w^2 m/(\hbar\pi s)$, is recovered. Thus, our theory reproduces the results of the previous approaches in the limiting case of a low electric field and strong carrier localization (small barrier tunneling coefficient).

C. Escape Time

The total carrier escape time is given as the ratio of the total escape flux J/e to the carrier density n as

$$\frac{1}{\tau} = \frac{J}{en} = \frac{\int_{E_0}^{\infty} j_E(E_z)\,dE_z}{n} \tag{18}$$

where the integral is taken over the whole range of energies E_z. This method gives the total tunneling escape time if the integration is restricted to the states below the barrier $E_z < E_B$, while the thermionic escape time is given by integration over energies above the barrier $E_z > E_B$.

Strictly speaking, to find the carrier density n, one can use the exact set of wavefunctions which can be obtained using the boundary conditions discussed previously. This procedure would yield the local density of states, and the total carrier density could then be calculated by integration over energy and an appropriate range of the z coordinate. This local density of states will be discussed elsewhere in connection with more complex systems where this method can give nontrivial results. However, in the case of a single QW with infinitely wide barriers as considered here, our simulations showed that the procedure of finding the local density of states could be circumvented without a significant loss of accuracy. Indeed, in the case of low barrier penetration, the 1-D density of quasi-bound states is a set of normalized Lorenz functions, with the energy width of each of them proportional to the tunneling coefficient and thus very small. Furthermore, it was found that, at room temperature, most carriers reside on the lowest well-bound states inside the QW. The local density of unbound states in the fast-tunneling region of energies or above the barrier is small and does not give a significant contribution to the total carrier density. Therefore, the

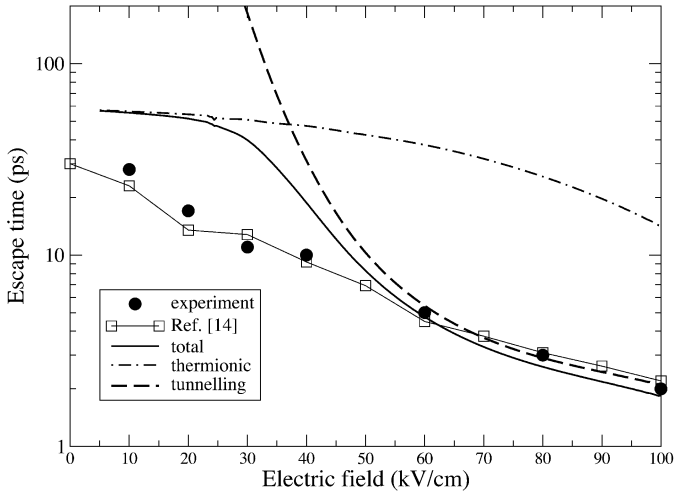

Fig. 2. Calculated and experimentally measured electron escape time from 9.6-nm GaAs QW as a function of the applied electric field. The solid, dashed, and dot–dashed curves show calculated total, thermionic, and tunneling escape times correspondingly. The experimental points (filled circles) are taken from Cavailles *et al.* [20] and the open squares are calculation results by Lefebvre and Anwar [13]. The detailed description of the model and experimental structures are given in the text.

latter can be accurately approximated by a sum of densities of carriers on well-localized quasi-bound levels

$$n_e = \sum_s P(E_s^{\mathrm{QB}}). \tag{19}$$

As the results of the next section show, the fact that unbound states give little contribution to the carrier density does not mean that the escape current due to these states is negligible. In fact, direct tunneling from the deeply localized states usually gives a very small contribution to the current, the major escape roots being through the upper states.

III. Results and Discussion

In this section, we present the results of calculations of electron escape time from a single GaAs QW at room temperature (300 K) for different applied electric fields, QW widths, and aluminum percentage x in $Al_xGa_{1-x}As$ barriers. The following material parameters for $Al_xGa_{1-x}As$ were used [19]: bandgap energy $E_g = 1.424 + 1.247x$ and electron effective mass $m_e = 0.067 + 0.083x$. The band offset ratio between GaAs and AlGaAs was taken as 67/33.

A. Comparison With Experimental Results for Electrons

In Fig. 2, the theoretical simulations are compared to measured electron escape times taken from Cavailles *et al.* [20]. Their paper reports, to our knowledge, the only available experimental work in which the electron and hole escape times were measured separately. This was achieved by means of a special asymmetric design: the structure $Al_{0.2}Ga_{0.8}As$–GaAs–$Al_{0.4}Ga_{0.6}As$ with the widths 20 nm/9.6 nm/20 nm was placed between the buffers with 30% of aluminum. As a result, one type of carriers faced a much higher potential barrier than the other, which allowed the escape processes of electrons and holes to be distinguished.

One can see that our simple semi-analytical theory gives values of the escape times that are reasonably close to the experimental points. The results of Lefebvre and Anwar [13] (open squares in Fig. 2) were obtained for an asymmetric structure with barriers of finite widths, which is exactly the same as in [20]. In our work, we have assumed symmetric barriers of infinite widths (the generalization of this theory for arbitrary design is fairly trivial and will be reported elsewhere), and it is reasonable to compare experimental results with the simulation of a symmetric QW with $Al_{0.2}Ga_{0.8}As$ barriers, since in an asymmetric structure the carriers escape chiefly toward the lower barrier with the higher barrier acting mainly as a carrier reflector, similarly to the infinite $Al_{0.2}Ga_{0.8}As$ barrier in our model. Still, we find that, at low electron fields, the calculations of Lefebvre and Anwar describe the structure of [20] more accurately than ours. This is not surprising as in this case the finite widths of the barriers may play an important role. At large fields, our theory (which is computationally much simpler than that of Lefebvre and Anwar) shows an agreement with experiment which is about as good as that of [13], despite analyzing a slightly simplified structure.

Decomposition of the escape time into the thermionic and tunneling components shows that, for a low electric field, the thermionic component is the main one, since the tunneling is slow, and, for a higher field, in this structure, the tunneling is predominant.

B. Comparison With Experimental Results for Holes

Our theory employs the simple single-band effective mass approximation, which is fairly accurate for electrons. In the case of holes, the band mixing leads to strong nonporabalicity for subbands inside the QW [21], as well as light-to-heavy hole (or vice versa) transformation in process of tunneling [22], which can significantly influence the carrier escape. To our knowledge, there has been no systematic study of the impact of band mixing on the hole escape; this will be the subject of our future work. Nevertheless, it is useful to test the applicability of the current simple theory to hole escape, since it is obvious that a rigorous theory taking into account the band mixing effects will be much more complicated than this one.

The transverse effective masses in $Al_xGa_{1-x}As$ for light (heavy) holes, $m_\perp^{lh} = 0.087 + 0.063 * x$ ($m_\perp^{hh} = 0.62 + 0.14 * x$) [19], are used to calculate reflection and transmission coefficients. The $\boldsymbol{k \cdot p}$ calculations show [21] that the band mixing effects lead to almost flat or even electron-like (negative mass) light-hole dispersion on the ground quantized level. As proposed in [20], in order to account for this, the following in-plane masses are taken: $m_{||}^{\mathrm{lh}} = 4.0$ for light holes and $m_{||}^{\mathrm{hh}} = 0.24$ for heavy holes. It is important to note that, if the in-plane mass is taken to be energy-independent (i.e., the same for all bound and unbound states), then the escape time for the particular type of particles will not depend on the value of the in-plane effective mass. Indeed, the escape current density (13), as well as carrier density (12), are proportional to the in-plane mass, thus it will cancel when the ratio (18) is taken.

In Fig. 3, the escape time calculated for constant in-plane hole masses is shown as a solid curve. The results are about an

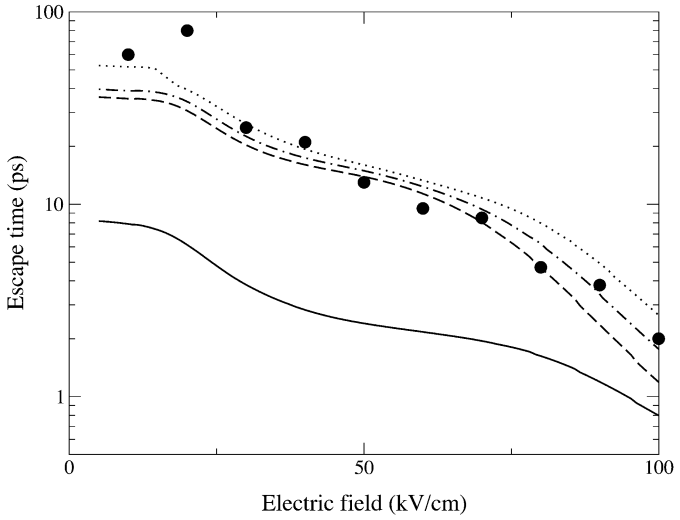

Fig. 3. Calculated and experimentally measured hole escape time from a 9.6-nm GaAs QW as a function of the applied electric field. The solid ($m_{\|}^{*}=4$, $m_{B}^{*}=0.099$), dashed ($m_{\|}^{*}=0.087$, $m_{B}^{*}=0.099$), dotted ($m_{\|}^{*}=0.087$, $m_{B}^{*}=0.646$) and dash–dotted ($m_{\|}^{*}=0.087$, $m_{B}^{*}=0.2$) curves show escape time for different effective-mass parameters (see details in the text). The experimental points (filled circles) are taken from Cavailles *et al.* [20].

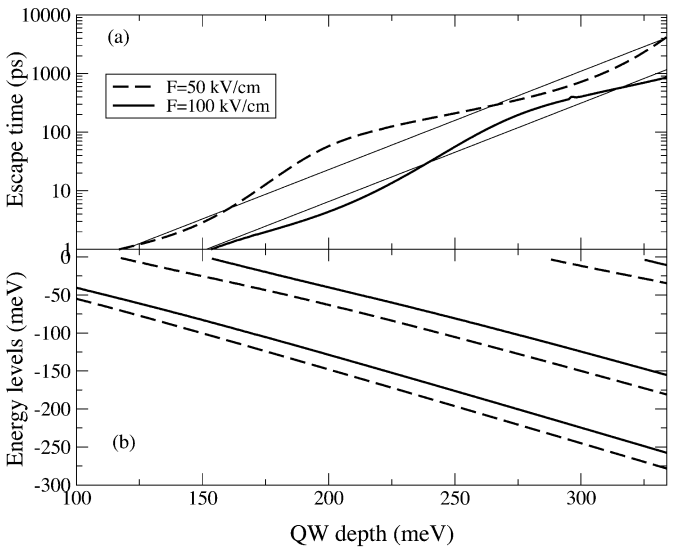

Fig. 4. Calculated (a) electron escape time and (b) quantized electron levels as a function of the QW depth $E_b - E_0$. The solid thick (dashed) lines correspond to the applied electric field of 100 kV/cm (50 kV/cm). The thin lines in (a) describe simple thermal activation law $\tau \propto \exp((E_b - E_0)/(kT))$.

order of magnitude lower than the experimental values. They are also lower than the electron escape time (Fig. 2), which is not surprising, since the barrier hight for holes is much lower than for electrons whilst the difference between the electron and light-hole barrier masses is only modest.

The above suggests that the assumption of a constant in-plane mass should be discarded. Indeed, it is clear that the effective mass above the barrier should coincide with that of the bulk case and taking the large light-hole effective mass is not justified.

To account for this, we keep the large in-plane mass (4.0) for quasi-bound light-hole levels, whereas the in-plane mass $m_{\|}^{*}$ for upper levels is taken to be equal to the bulk value of 0.087. (The heavy holes mass is kept unchanged here and below, for the sake of simplicity.) The results, shown as the dashed curve in Fig. 3, prove a significantly better ability of such an approach to describe the experimental results.

We roughly assess the influence of the light-to-heavy hole conversion in the process of tunneling by taking the value of light-hole barrier mass m_{B}^{*} to be in between the bulk light (0.099) and heavy (0.646) masses. When the mass m_{B}^{*} is taken to be 0.646 (the dotted curve in Fig. 3, 100% conversion from light to heavy holes), the increase of the escape time is noticeable but not crucial. The best overall fit to experimental results is achieved for the mean value of $m_{B}^{*}=0.2$.

To conclude this section, it appears that the strong valence subband mixing in a QW plays the prime role for the escape processes and can be described in the first approximation by taking enhanced in-plane effective mass for quasi-bound levels while retaining the bulk effective mass for the unbound levels. A more accurate multiband $\boldsymbol{k}\cdot\boldsymbol{p}$ theory for carrier escape would be preferable for detailed quantitative analysis; this is reserved for future work.

C. Dependence of the Escape Time on QW Parameters

In what follows, we examine the dependence of electron escape time on the barrier composition (QW depth) and the QW width. Fig. 4(a) shows the dependence of the escape time on the conduction band offset between the QW and the barrier $E_b - E_0$ for two different applied fields. A simple thermal activation dependence $\tau \propto \exp((E_b - E_0)/(kT))$ is depicted by thin lines. One can see that the overall character of escape time increase with the QW depth is exponential with the average growth constant of about β, which suggests that thermal activation is the main escape mechanism in this case. The same conclusion was drawn previously from a study of a single-QW waveguide modulator [12]. However, the exact dependence of the escape time on the QW depth exhibits significant variations from the simple exponential law. One can see that there are significant correlations between the dependence character and the energy position of the electron quantized levels [see Fig. 4(b)]. The electron levels in Fig. 4(b) are calculated using (14) and are measured from the QW edge E_b. Just before and straight after the appearance of a new electron level in the QW, the escape time increase becomes slower, whereas when the QW level deepens the escape time increases even faster than $\exp((E_b - E_0)/kT)$.

In Fig. 5(a), the escape time as a function of the QW width is shown.

Our results differ qualitatively from those given by the simple formula by Schneider and von Klitzing [7]. Indeed, the well width behavior of the escape times is almost periodic, with several maxima and minima. An appropriate use of this dependence can be potentially crucial for device applications. Indeed, as can be seen from Fig. 5(a), an increase of the QW width from 8.2 to 11.3 nm decreases the value of the electron escape time by a factor of four.

Analyzing Fig. 5(a) in connection with Fig. 5(b), one can deduce that the occurrence of maxima and minima in different

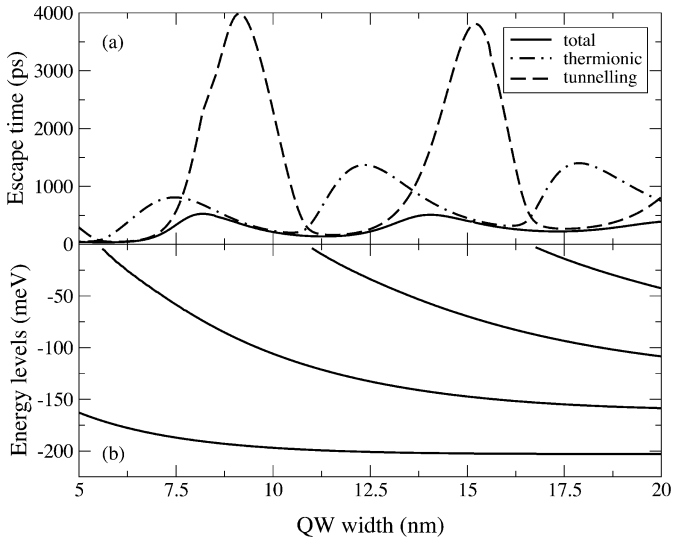

Fig. 5. (a) Electron escape time and (b) electron levels for a QW with $Al_{0.3}Ga_{0.7}As$ barriers and applied electric filed $F = 50$ kV/cm as a function of QW width.

components of escape time are strongly correlated with the energy position of electron eigen-levels in the QW. The crossovers between thermionic and tunneling times at $w = 5.5$, 10.8, and 16.6 nm approximately coincide with the appearance of new eigen-levels in the QW.

When a new eigenstate appears, the escape is dominated by tunneling, which suggests that the main route of escape goes through a "newborn" state. An even more surprising feature is that the thermionic escape time "feels" the advent of the new state. Before the new state appears, the thermionic time decreases, indicating the increase of the escape current through the states above the barrier. As the state becomes more localized, the tunneling rate decreases, and, eventually, thermionic emission overcomes tunneling.

In order to investigate the apparent connection between the QW quantized states and the escape time behavior, we show (Fig. 6) the energy density of the flux of escaping electrons (13), as a function of $E_z - E_b$ for different QW widths in the vicinity of the width at which a new QW electron eigenstate appears, $w \approx 10.5$ nm [see Fig. 5(b)]. One can see that, just before the eigenstate appears, there is a significant flux-density enhancement in the region above the barrier $E_z - E_b > 0$, with a broad peak centered in this energy area (see the curve for $w = 10$ nm). This escape enhancement for upper states is responsible for the decrease in the value of the thermionic escape time before the new eigen state appears. This shows that the nonzero reflection coefficient for electron waves above the barrier ensures a continuity between the states above the barrier (extended states) and states deep in the QW (quasi-bound states). In this respect, the decomposition of the escape time into the thermionic and tunneling components becomes somewhat artificial.

As the QW broadens ($w = 11$, 12 nm), the flux-density peak moves under the barrier and becomes narrower. One should notice, however, that the significant tunneling current is accompanied by a significant broadening of the eigenstate. In this case ($w = 11$, 12 nm), the newly appeared state still cannot be treated as a quasi-bound one due to its large broadening. On the other

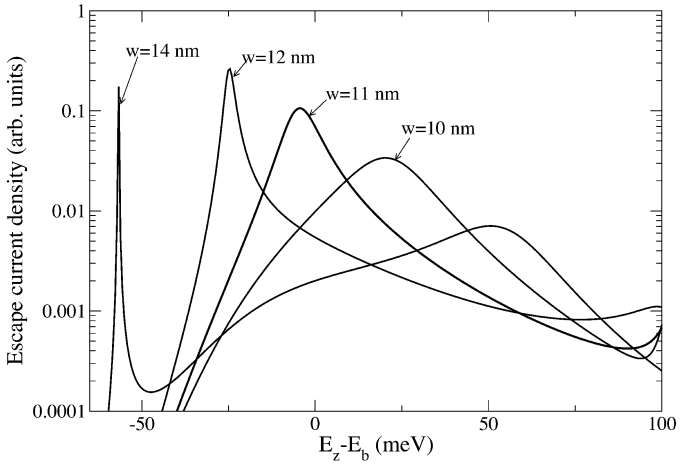

Fig. 6. Energy density of escape electron flux for different QW widths $w = 10$, 11, 12, and 14 nm. The aluminum composition in the barriers and the applied electric field are the same as for Fig. 5.

hand, deep states like that for $w = 14$ nm and deeper give a small contribution to the escape current. Indeed, a careful examination of the narrow flux-density peaks around these states shows that the calculated tunneling time from a quasi-bound state coincides with those given by (16) and (17) to a high precision and is generally large due to the small transition coefficient.

Thus, we found that the main contribution to carrier escape arises from the states in the energy interval near the barrier edge (see Fig. 6). Therefore, the escape process can be characterized as thermally assisted tunneling/emission through near-barrier-edge states. The states in this energy interval possess a mixed character, intermediate between purely 3-D states high in the conduction band and the quasi-2-D character of QW quantized states. This suggests that those theoretical methods that use an artificial separation of escape processes into quasi-2-D tunneling and quasi-3-D thermionic emission, which fails in this very energy region, are not very reliable when used for a quantitative study of semiconductor saturable absorbers.

A practical recommendation for the saturable absorber design can be drawn from the above computational modeling: in order to minimize the carrier escape time, one should adjust the QW width so that for the intended operational bias, a shallow eigenstate exists or is about to appear. A more significant improvement may be achieved by using more complex structures than a single abrupt QW; the application of our theory to the design of such structures will be reported elsewhere [23].

IV. Conclusion

The dependence of the escape time from a single QW on the applied electric field and QW depth and width is analyzed by means of a new simple, yet relatively accurate, theory. A good agreement with experimental results is established. The main escape process is found to be thermally assisted tunneling/emission through near-barrier-edge states.

Acknowledgment

The authors would like to thank I. A. Larkin for valuable discussions and advice.

REFERENCES

[1] S. Hojfeldt and J. Mørk, "Modeling of carrier dynamics in quantum-well electroabsorption modulator," *IEEE J. Select. Topics Quantum Electron.*, vol. 8, pp. 1265–1276, 2002.

[2] A. Larson, P. A. Andrekson, S. T. Eng, and A. Yariv, "Tunable superlattice p-i-n photodetectors: Characteristics, theory, and applications," *IEEE J. Quantum Electron.*, vol. 24, pp. 787–801, 1988.

[3] E. A. Avrutin, J. H. Marsh, and E. L. Portnoi, "Monolithic and multi-gigahertz mode-locked semiconductor lasers: Constructions, experiment, models and applications," *Proc. Inst. Elect. Eng.*, pt. J, vol. 147, pp. 251–278, 2000.

[4] H. Kurita, I. Ogura, and H. Yokoyama, "Ultrafast all-optical signal processing with mode-locked semiconductor lasers," *IEICE Trans. Electron.*, vol. E81C, pp. 129–139, 1998.

[5] C. Knöll, M. Golles, Z. Bakonyi, G. Onishchukov, and F. Lederer, "Optimization of signal transmission by an inline semiconductor amplifier-saturable absorber module," *Opt. Commun.*, vol. 187, pp. 141–153, 2001.

[6] F.Öhman, S. Bischoff, B. Tromborg, and J. Mørk, "Noise properties and cascadability of soa-ea regenerators," *Proc. 15th Annu. Meeting IEEE Lasers and Electro-Optics Soc.*, pp. 895–896, Nov. 2002.

[7] H. Schneider and K. v. Klitzing, "Thermionic emission and Gaussian transport of holes in a GaAs/$Al_xGa_{1-x}As$," *Phys. Rev. B*, vol. 38, pp. 6160–6165, 1988.

[8] D. Ahn and S. L. Chuang, "Exact calculations of quasibound states of an isolated quantum well with uniform electric field: Quantum-well Stark resonance," *Phys. Rev. B*, vol. 34, pp. 9034–9037, 1986.

[9] D. C. Hutchings, "Transfer matrix approach to the analysis of an arbitrary quantum well structure in an electric field," *Phys. Rev. B*, vol. 34, pp. 9034–9037, 1986.

[10] V. J. Goldman, D. C. Tsui, and J. E. Cunningham, "Resonant tunneling in magnetic fields: Evidence for space-charge buildup," *Phys. Rev. B*, vol. 50, pp. 10 864–10 967, 1994.

[11] D. J. Moss, T. Ido, and H. Sano, "Calculation of photogenerated carrier escape rates from GaAs/$Al_xGa_{1-x}As$ quantum wells," *IEEE J. Quantum Electron.*, vol. 30, pp. 1015–1026, 1994.

[12] R. Bambha, D. C. Hutchings, M. J. Snelling, P. Likamwa, A. Miller, A. L. Moretti, R. W. Wickman, K. A. Stair, T. E. Bird, J. A. Cavailles, and D. A. B. Miller, "Carrier escape dynamics in a single quantum well waveguide modulator," *Opt. Quantum Electron.*, vol. 25, pp. S965–S971, 1993.

[13] K. R. Lefebvre and A. F. M. Anwar, "Electron escape time from single quantum wells," *IEEE J. Quantum Electron.*, vol. 33, pp. 187–191, 1997.

[14] A. F. M. Anwar and K. R. Lefebvre, "Electron escape via polar optical-phonon interaction and tunneling from biased quantum wells," *Phys. Rev. B*, vol. 57, pp. 4584–4590, 1998.

[15] M. J. McLennan, Y. Lee, and S. Datta, "Voltage drop in mesoscopic systems: A numerical study using a quantum kinetic equation," *Phys. Rev. B*, vol. 43, pp. 13 846–13 883, 1991.

[16] A. F. M. Anwar and M. M. Jahan, "Density of states for double-barrier quantum-well structures under the influence of external fields and phase-braking scattering," *Phys. Rev. B*, vol. 50, pp. 10 864–10 967, 1994.

[17] G. E. Andrews, R. Askey, and R. Roy, *Special Functions*, 1st ed. Cambridge, U.K.: Cambridge Univ. Press, 1999, p. 78.

[18] L. D. Landau and E. M. Lifshitz, *Quantum Mechanics*, 2nd ed. Oxford, U.K.: Pergamon Press, 1965, p. 78.

[19] S. Adachi, "GaAs, AlAs and $Al_xGa_{1-x}As$: Material parameters for use in research and device applications," *J. Appl. Phys.*, vol. 58, pp. R1–R29, 1985.

[20] J. A. Cavailles, D. A. B. Miller, J. E. Cunningham, P. L. KamWa, and A. Miller, "Simultaneous measurements of electron and hole sweepout from quantum wells and modeling of photoinduced field screening dynamics," *IEEE J. Quantum Electron.*, vol. 28, pp. 2486–2497, 1992.

[21] L. C. Andreani, A. Pasquarello, and F. Bassani, "Hole subbands in strained GaAs/$Ga_{1-x}Al_xAs$ quantum wells: Exact solution of the effective-mass equation," *Phys. Rev. B*, vol. 36, pp. 5887–5894, 1987.

[22] S. L. Chuang, "Theory of hole refractions from heterojunctions," *Phys. Rev. B*, vol. 40, pp. 10 379–10 390, 1989.

[23] V. V. Nikolaev and E. A. Avrutin, "Quantum-well design for monolithic optical devices with gain and saturable absorber sections," *IEEE Photon. Technol. Lett.*, to be published.

Valentin V. Nikolaev was born in St. Petersburg (then Leningrad), Russia, in 1978. He received the M.Sc. degree with distinction from St. Petersburg State Technical University, Russia, in 2001 and the Ph.D. degree from the University of Exeter, U.K., in 2002.

Since September 2002, he has been working at the Department of Electronics, University of York, York, U.K., on a research project aimed at developing theoretical understanding of novel optoelectronic devices.

Eugene A. Avrutin (M'95) was born in St. Petersburg (then Leningrad), Russia, in 1963. He received the M.Sc. degree with distinction from St. Petersburg Technical University (then Leningrad Polytechnical Insitute), Russia, in 1986 and the Ph.D. degree from A.F. Ioffe Physico-Technical Institute, St. Petersburg, in 1994.

From 1986 to 1993, he was with the Integrated Optics Laboratory, A.F. Ioffe Physico-Technical Institute, and from 1994 to 1999 with the Department of Electrical and Electronic Engineering, University of Glasgow, Glasgow, U.K. Since 2000, he has been a Lecturer at the Department of Electronics, University of York, York, U.K., where his interests are in theory, modeling, and design of optoelectronic devices and in advancement of photonic CAD techniques.